Observational Study

Medicine

OPEN

A bioinformatics and experimental study toward new therapeutic strategies

CXCL8 in gout progression

Chao Zhang, MS[a], Chunhong Liu, MS[b], Xiaoming Yang, MS[b], Xin Lin, MS[b], Miao Wang, MS[b], Yanlang Yang, PhD[b,*]

Abstract

Gout is a chronic inflammatory disease driven by hyperuricemia and recurrent immune activation. However, gout may occur in the absence of elevated serum uric acid levels, which complicates clinical diagnosis and highlights the need for reliable molecular biomarkers. The molecular mechanisms underlying gout progression remain incompletely understood. This observational study integrated bioinformatics analyses with experimental validation. Publicly available transcriptomic datasets were analyzed to identify differentially expressed genes between gout patients and healthy controls. Functional enrichment analysis, protein–protein interaction network construction, immune cell infiltration analysis, competing endogenous RNA network analysis, and gene set enrichment analysis were performed to explore C-X-C motif chemokine ligand 8 (*CXCL8*)-associated molecular pathways. In vitro experiments were conducted to evaluate hyperuricemia-induced inflammatory responses in renal cells. A total of 1848 differentially expressed genes were identified, which were predominantly enriched in immune and inflammatory regulatory pathways. Five hub genes were highlighted, among which *CXCL8* emerged as a key mediator of immune cell activation. Gene set enrichment analysis revealed that *CXCL8* was significantly associated with inflammatory signaling pathways, including the NOD-like receptor signaling pathway. Potential upstream regulators of *CXCL8* were also identified. Experimental validation demonstrated that elevated uric acid levels induced renal cell injury and inflammatory responses, accompanied by increased *CXCL8* expression and activation of the NOD-like receptor family pyrin domain containing 3 inflammasome pathway. This study preliminarily identifies *CXCL8* as a critical inflammatory mediator involved in gout progression and suggests its potential value as a molecular biomarker and therapeutic target, providing a basis for future diagnostic and therapeutic strategies.

Abbreviations: ceRNA = competing endogenous RNA, CXCL8 = C-X-C motif chemokine ligand 8, DEG = differentially expressed genes, GEO = Gene Expression Omnibus, GO_BP = gene ontology biological process, GSEA = gene set enrichment analysis, KEGG = kyoto encyclopedia of genes and genomes, MSU = monosodium urate, NGS = next-generation sequencing, NLRP3 = NOD-like receptor family pyrin domain containing 3, PPI = protein–protein interaction, sUA = serum uric acid, UA = uric acid.

Keywords: biomarker, comprehensive analysis, *CXCL8*, GOUT, hyperuricemia, inflammation

1. Introduction

Gout is a common auto-inflammatory joint disorder typically characterized by acute, painful episodes of arthritis caused by the deposition of monosodium urate (MSU) crystals in the joints and surrounding tissues.[1] A major risk factor for gout is hyperuricemia, a condition marked by elevated serum uric acid (sUA) levels, which is defined as fasting sUA concentrations above 420 μmol/L (7 mg/dL).[2] Numerous epidemiological studies have demonstrated that hyperuricemia significantly elevates the risk of developing gout, and that sUA levels act as independent risk factors for gout, with the likelihood of gout events increasing non-linearly with higher sUA concentrations.[3] For example, in the normative ageing study, the cumulative incidence of gout over 15 years was found to range from 1.1% at an

This study was supported by the Talents of Scientific Research Fund Program from Yijishan Hospital Affiliated Wannan Medical School (YR201918) and the Horizontal Research Fund of Wannan Medical College (Grant No. 662202404013).

The authors have no conflicts of interest to disclose.

The datasets generated during and/or analyzed during the current study are publicly available.

All data used in this work are openly accessible online and received informed consent from participants, ethical approval from the relevant institutional review boards, and strict quality control, as mentioned in the manuscript. The manuscript does not contain clinical trials or patient data, and all data used in this study are publicly available, so ethical approval was not required.

[a] Department of Nephrology, Tongling Hospital of Traditional Chinese Medicine, Tongling, Anhui, China, [b] Department of Nephrology, Yijishan Hospital of Wannan Medical College, Wuhu, Anhui, China.

** Correspondence: Yanlang Yang, Department of Nephrology, Yijishan Hospital of Wannan Medical College, No. 92 Zheshan West Road, Jinghu District, Wuhu 241000, Anhui, China (e-mail: yangyanlang@126.com).*

How to cite this article: Zhang C, Liu C, Yang X, Lin X, Wang M, Yang Y. A bioinformatics and experimental study toward new therapeutic strategies: CXCL8 in gout progression. Medicine 2026;105:10(e47873).

Received: 9 January 2025 / Received in final form: 16 January 2026 / Accepted: 10 February 2026

http://dx.doi.org/10.1097/MD.0000000000047873

sUA concentration of 6 mg/dL to 49% at 10 mg/dL.[4] Similarly, the Malmö Prevention Project revealed that the absolute risk of gout after a 30-year follow-up was 3.8%, but increased dramatically to 14% to 20% in individuals with hyperuricemia.[5] Although the strong association between hyperuricemia and gout is well established, predicting who will develop gout remains clinically challenging. Approximately half of individuals with sUA concentrations ≥10 mg/dL will develop clinically significant gout within 15 years, underscoring the importance of identifying high-risk patients and implementing targeted preventive measures.[4]

Gout is now recognized as a multifaceted disease with symptoms that extend beyond local inflammation, reflecting a more complex pathology than previously thought. It is no longer regarded merely as a joint ailment but as a systemic disorder involving metabolic dysregulation and chronic inflammation.[6] Both genetic and environmental factors contribute to the risk of developing gout, with hyperuricemia being the most significant.[7] Elevated sUA levels greatly increase the likelihood of gout attacks, and the association between sUA concentrations and gout risk is concentration-dependent. As sUA concentrations rise, the risk of gout increases sharply. The progression of gout typically follows a sequence, starting with hyperuricemia without MSU crystal deposition, then advancing to crystal deposits in asymptomatic hyperuricemia, followed by episodes of acute gout, and eventually developing into chronic gouty arthritis.[8] Recognizing each stage of this progression allows for timely interventions that can mitigate long-term damage.

Given the complex nature of gout and its systemic effects, exploring the genetic factors involved becomes essential.[9] Therefore, screening and studying gout-related genes can significantly enhance our understanding of cellular adaptations under high UA conditions. By investigating the molecular mechanisms involved, we can improve our ability to predict and manage chronic inflammatory diseases like gout. Such research could provide valuable insights into potential protective strategies and therapeutic targets for conditions where chronic inflammation plays a central role, paving the way for more effective prevention and treatment of gout and related diseases.[10] Ultimately, this could pave the way for more effective prevention and treatment options for gout and related diseases, improving patient outcomes and quality of life.

Microarray and high-throughput sequencing technologies have revolutionized disease diagnosis, with next-generation sequencing (NGS) standing out as a critical tool, especially in the study of renal disorders.[11] In conditions like autosomal dominant polycystic kidney disease, NGS is instrumental in identifying potential genetic mutations, discovering biological targets, and offering clinically relevant diagnostic insights for both typical and atypical genetic cases, such as those involving allele variations, gene interactions, somatic chimerism, or modifiers of cystic kidney disease.[12,13] Recent advancements in bioinformatics, an interdisciplinary field connecting computer science, information technology, and biology, are crucial in managing the vast datasets generated by these high-throughput platforms.[14] The integration of NGS and bioinformatics facilitates efficient data processing and interpretation, which has become indispensable in analyzing biological sequences, as well as in genomics, transcriptomics, proteomics, metabolomics, and systems biology.[15]

Despite the growing body of bioinformatics research in renal tumors and hereditary kidney diseases, there remains a notable paucity of studies on hyperuricemia and its progression to GOUT. This knowledge gap makes it challenging to identify reliable biomarkers capable of distinguishing or predicting the transition from hyperuricemia to GOUT. As a result, atypical presentations of GOUT are often misdiagnosed, or diagnosis is delayed, complicating clinical management.[16] To address this gap, we analyzed NGS data (GSE160170) uploaded to the Gene Expression Omnibus (GEO) database by Qing et al Differentially expressed genes (DEGs) were identified between gout-afflicted and healthy peripheral blood samples, followed by enrichment analysis for the gene ontology biological process and kyoto encyclopedia of genes and genomes (KEGG) signaling pathways. Our goal was to provide insights into the molecular mechanisms underpinning tissue damage and physiological adaptation under hyperuricaemic conditions. Preliminary bioinformatics analyses revealed significant upregulation of the C-X-C motif chemokine ligand 8 (*CXCL8*) gene, a key node in the protein–protein interaction (PPI) network. Chemokines, particularly those of the CXC family, are pivotal mediators of neutrophil recruitment and inflammation in crystal-induced arthritis, including gout. *CXCL8* encodes a protein belonging to the CXC chemokine family, commonly referred to as interleukin-8.[17] *CXCL8* is a crucial modulator of the inflammatory response and is secreted by a range of cell types, including mononuclear macrophages, neutrophils, eosinophils, T lymphocytes, epithelial cells, and fibroblasts.[18] It is particularly active under environmental stressors, such as exposure to proinflammatory cytokines, UV irradiation, and ischemic or hypoxic conditions.[19] While *CXCL8* has been extensively studied in the context of other inflammatory diseases, its role in hyperuricemia and GOUT remains largely unexplored.[20] Given the pivotal function of *CXCL8* in mediating cellular inflammatory damage, further research is warranted to elucidate the precise mechanisms by which *CXCL8* contributes to inflammation and injury in hyperuricemia-induced pathologies. Unraveling this relationship could offer new avenues for early diagnosis and therapeutic intervention in GOUT.

This study utilized bioinformatics techniques to analyze GEO data obtained from microarray technology, with a focus on investigating immune cell infiltration and competing endogenous RNA (ceRNA) networks in patients with primary gout. By doing so, the research sheds light on the molecular mechanisms of gout-related genes and identifies key biomarkers. To further support these findings, in vitro experiments were performed to assess and compare the expression of key regulatory factors associated with hyperuricemia-related genes. These experiments provide a preliminary foundation for identifying potential biomarkers that may help distinguish or predict the transition from hyperuricemia to gout, warranting further validation.

2. Materials and methods

2.1. Bioinformatics analysis of differentially expressed genes in the peripheral blood of GOUT patients

2.1.1. Data selection. The GSE160170 dataset, which included 6 gout samples and 6 normal samples for subsequent analysis, was downloaded from the National Center for Biotechnology Information Gene Expression Omnibus (NCBI-GEO; http://www.ncbi.nlm.nih.gov/geo). The platform for the dataset was GPL21827 Agilent-079487 Arraystar Human LncRNA microarray V4 (probe name version).

2.1.2. Data processing. To obtain the expression matrix dataset needed for this project in the form of a subset, the data were cleaned and quality controlled using software in R language, such as tidyverse, GEOquery, and stringr. Next, the clinical information of the corresponding samples was collected in accordance with the expression matrix data samples for further sample classification, after which the gene IDs were converted using AnnoProbe software in R language. Finally, the differential expression analysis of the 2 groups of samples was performed using the limma R package to filter out genes with a difference multiple >1-fold and write the gene name annotation information. After analyzing the data, we obtained normal samples (6 cases) to use as the control group and GOUT samples (6 cases) to use as the treatment group by utilizing |logFC|>1 and adjusting $P < .05$ to evaluate the degree of GOUT.

2.1.3. Enrichment analysis. The gene names (SYMBOL) in the data were converted to ENTREZID using the org.Hs.e.g.db software in R language, and the DEGs were than subjected to gene ontology biological process[21] and KEGG analyses[22] using the enrichment analysis software clusterProfiler to determine the biological significance of DEG enrichment. $P < .05$ was the selection criterion for GO enrichment analysis and $P < .05$ was the selection criterion for KEGG pathway analysis.

2.1.4. Protein interactions and network correlation analysis. The Search Tool for the Retrieval of Interacting Genes/Proteins (STRING) is an online database and analysis software for retrieving known interactions between genes (proteins) and predicted genes (proteins). To evaluate the interactions between DEGs, this study used the STRING analysis results as a basis for network association analysis of these genes.

2.1.4.1. Protein interaction analysis. To form the PPI network, the screened differential genes were entered into STRING (https://string-db.org/cgi/input.pl; version 11.0)[23] in the multiple proteins entry box, and *Homo sapiens* was selected in the organism entry box, using high confidence (0.7) protein interaction source as the default setting to remove isolated and partially connected nodes.

2.1.4.2. Gene (protein) network correlation analysis. The obtained protein interaction data were imported into Cytoscape network analysis software (version 3.8.0),[24] and the NetworkAnalyzer Tool (version 5.11.2)was used to calculate the degree of association (degree) between nodes (genes), find HUB genes located in the center of the network, and draw a network interaction map.

2.1.5. Immune infiltration analysis. To calculate immune infiltration, we used the web-based tool CIBERSORT,[25] which is a deconvolution method. This method can evaluate the ratio of 22 different infiltrating lymphocyte subsets across a large number of tissue samples. GraphPad Prism 8.0.2 (San Diego)[26] was employed for the correlation analysis between the different immune cells as well as between immune cells and the hub genes to calculate the ratio of each immune cell subset detected in GOUT tissues compared to controls.

2.1.6. Exploration ceRNA network of the hub genes. Target miRNA identification for hub genes: potential miRNAs were identified for each of the 5 hub genes using TarBase, TargetScan and miRNet,[27,28] and the intersection of the predicted results from the 3 sites was taken to identify the target miRNA for each hub gene. lncRNA prediction and ceRNA pair identification: Using the miRNet website, the reciprocal lncRNAs of the miRNAs identified in the above results were identified, resulting in a total of 697 predicted lncRNAs. The intersection of these lncRNAs with differentially upregulated lncRNAs was taken, and 24 lncRNAs were obtained. The sequence information of these 24 lncRNAs was obtained using the NONCODE database, and the subcellular localization of lncRNAs was predicted using lncLocator. Ten lncRNAs localized in the cytoplasm were finally identified, mRNA-miRNA and miRNA-lncRNA were linked together by miRNA, and 30 ceRNA pairs were finally identified.

2.1.7. Gene set enrichment analysis. To investigate the potential molecular signaling route in which *CXCL8* is implicated in GOUT, the gene set enrichment analysis (GSEA) tool[29] was used. The official website's c2.cp.kegg.v7.3.symbols.gmt gene sets were employed in the pathway enrichment study.

2.2. Establishing a cellular model of hyperuricaemia

2.2.1. Reagents. Anti-NLRP3 (ab263899) antibody and anti-pro Caspase-1 + p10 + p12 (ab179515) antibody were purchased from Abcam, ASC (WL02462) antibody and CXCL8 (WL03074) antibody were purchased from Wanlei, and GAPDH (AC001) antibody was purchased from Abclonal. The CCK-8 kit was purchased from Ruijie (Anhui, China).

2.2.2. Establishment of a cell culture and injury model. Human renal tubular epithelial cells (HK-2 cells) were purchased from Guangzhou Saiku Biotechnology Co. HK-2 cells were cultured in vitro in DMEM/F-12 (Gibco, Grand Island) containing 10% fetal bovine serum (Gibco) and 1% penicillin/streptomycin (Gibco), and incubated at 37°C in a humidified atmosphere with 5% CO_2. Cells between passages 3 and 5 were used for all experiments to ensure consistency. For the hyperuricemia model, a stock solution of UA (Sigma-Aldrich, St. Louis) was prepared by dissolving in 0.1 M NaOH and adjusting the pH to 7.4 with HCl. The solution was then sterile-filtered and added to the culture medium to achieve the indicated final concentrations (0, 10, 20, 30, 40 mg/dL). Cells were treated for 48 hours and then collected for subsequent experiments.

2.2.3. Cellular viability. HK-2 cells in the logarithmic growth phase were inoculated in 96-well plates, with 10 replicate wells in each group, and incubated at 37°C in a 5% CO_2 saturated humidity incubator. After the cells were plated, the renal tubular epithelial cells were treated with 0, 10, 20, 30, and 40 mg/dL UA for 48 hours. The cells were cultured to the optimal state, and 10 μl of CCK8 working solution was added to each well and incubated at a constant temperature of 37°C for ~3 hours. The reacted 96-well plates were placed in an enzyme marker, and the OD values of the samples were detected at 450 nm.

2.2.4. Western blot analysis. Following the incubation and intervention, the cells were lysed in RIPA buffer containing 2% of a combination of protease and phosphatase inhibitors on ice for 20 minutes. After being sonicated, the samples were centrifuged at 4°C for 20 minutes, and the supernatants from each sample were saved for further use. The BCA protein assay kit was used to ascertain the total protein content. Using sodium dodecyl sulfate–polyacrylamide gel electrophoresis (SDS-PAGE) with either 10% or 12% protein concentration, equal quantities of protein (20 μg) were separated. The proteins that had been separated were then deposited electrophoretically onto polyvinylidene difluoride 9 (PVDF) membranes (Millipore, Billerica). After 2 hours of incubation with 5% nonfat milk powder in TBS buffer containing Tween (TBST) at room temperature, the samples were washed 3 times with TBST and then incubated with primary antibody at 4°C overnight. The membrane was washed one moretime, and then incubated with HRP-conjugated anti-rabbit IgG at room temperature for 1 hour. After washing with a chemiluminescent HRP substrate, the strips were then photographed using a chemiluminescence system (ChemiDocTM XRS + from Bio-Rad). The ImageJ program was used to perform a quantitative analysis on Western blot images. To verify equal protein loading, GAPDH analysis was performed.

2.3. Statistical analysis

All values are expressed as the means ± standard deviation. To determine whether there was a statistically significant difference between the groups, a 1-way analysis of variance was performed, and GraphPad Prism was then used to perform multiple comparisons. A statistically significant difference was considered when $P < .05$.

3. Results

3.1. Microarray data source and identification of differentially expressed genes

The protocol used throughout this study is shown in Figure 1. We downloaded the GSE160170 datasets from the GEO

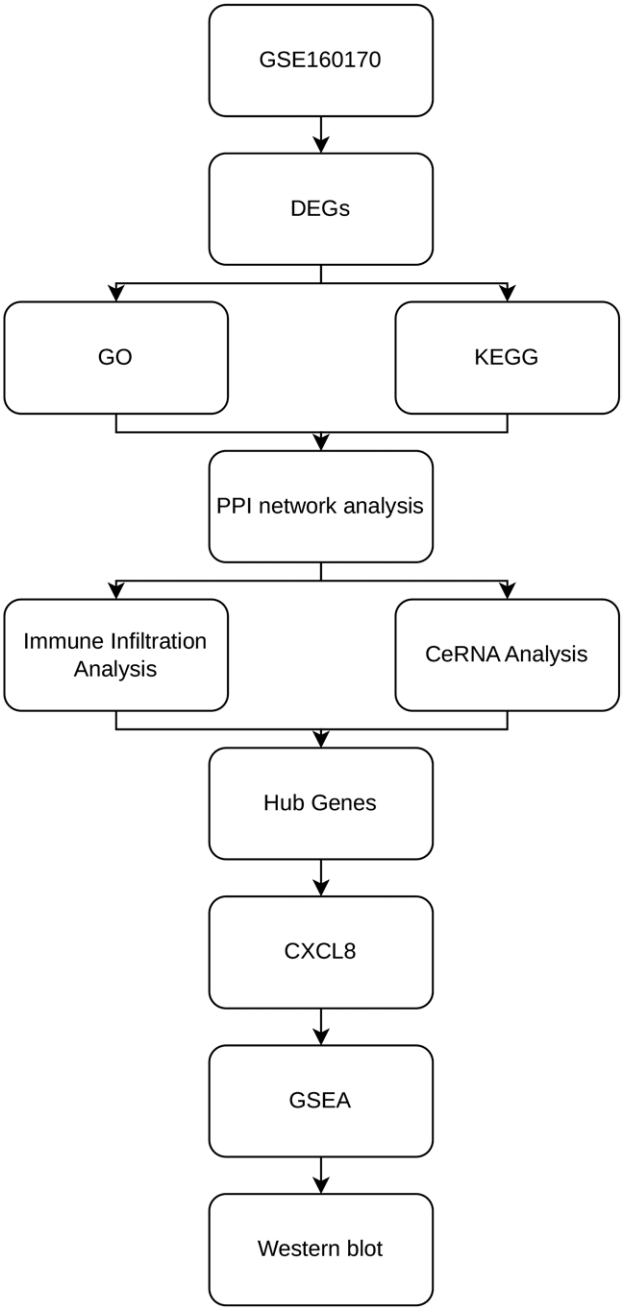

Figure 1. Flowchart of the study. ceRNA = competing endogenous RNA, CXCL8 = C-X-C motif chemokine ligand 8, DEG = differentially expressed gene, GO = gene ontology, GSEA = gene set enrichment analysis, KEGG = kyoto encyclopedia of genes and genomes, PPI = protein–protein interaction.

database, which contained primary gout (n = 6) and healthy subjects (n = 6). Comparative analysis revealed 1848 DEGs in gout patients compared to healthy controls, including 830 upregulated genes and 1018 downregulated genes. Figure 2A shows a heatmap of these differential genes, and Figure 2B presents a volcano plot of the 1848 DEGs, demonstrating significant transcriptional differences between the gout and control groups.

3.2. Functional enrichment analysis of DEGs

To clarify the biological functions and signaling pathways involved, we performed GO and KEGG enrichment analysis on the DEGs using clusterProfiler. GO enrichment analysis showed that 815 DEGs were enriched in 127 biological processes, such as leucocyte chemotaxis, regulation of chemotaxis, alpha-beta T cell activation involved in immune response, and regulation of stress-activated MAPK cascade (Table 1, Fig. 3). KEGG signaling pathway enrichment Analysis indicated that 397 DEGs were present in 308 pathways, including Herpes simplex virus 1 infection, Toll-like receptor signaling pathway, NOD-like receptor signaling pathway, MAPK signaling pathway, and p53 signaling pathway (Fig. 4).

3.3. PPI network construction and hub gene identification

We applied the STRING database and Cytoscape software to construct a PPI network of the DEGs, which consisted of 292 nodes and 1444 edges (Fig. 5A). Using the MCODE plugin, the top module was identified with a score of 11.7, containing 13 nodes and 140 edges (Fig. 5B). Subsequently, cytoHubba analysis using the degree, betweenness, MNC, and MCC algorithms consistently identified 5 central HUB genes: *TNF*, *JUN*, *IL4*, *CXCL8*, and *VEGFA* (Table 2, Fig. 5C).

3.4. Immune infiltration landscape in gout

To examine the immune context, we used the CIBERSORT algorithm to compare immune cell profiles between gout patients and controls. Figure 6A illustrates the proportions of 17 immune cell types across samples, and Figure 6B displays the correlation matrix between these cells. Quantitative comparison revealed that in GOUT, the percentage of activated Mast cells was substantially greater than in controls, whereas the proportions of T cells CD4 naive, NK cells resting, Macrophages M2 and Mast cells resting were significantly lower (Fig. 6C). Pearson correlation analysis further delineated the relationship between these immune cells and the HUB genes. A positive correlation was found between Mast cells activated and levels of *CXCL8*, *JUN*, *VEGFA*, and *TNF*, while a negative correlation was observed with *IL-4*. Conversely, T cells CD4 naive were positively correlated with IL-4 but negatively correlated with *CXCL8*, *JUN*, *VEGFA* and *TNF* (Fig. 6D).

3.5. Construction of an mRNA-miRNA-lncRNA ceRNA network

We explored the post-transcriptional regulatory network involving the hub genes. Potential miRNAs targeting each hub gene were identified using TarBase, TargetScan, and miRNet, taking the intersection of predictions. This yielded 30 miRNAs for *CXCL8*, 24 for *JUN*, 1 for *TNF*, and 61 for *VEGFA*, forming 118 mRNA-miRNA interaction pairs overall (Fig. 7A). Reciprocal lncRNAs for these miRNAs were predicted via miRNet, resulting in 697 candidates. Intersection with differentially upregulated lncRNAs yielded 24 lncRNAs. Using lncLocator to predict subcellular localization, 10 lncRNAs localized in the cytoplasm were finalized: UCA1, LINC01433, KCTD21-AS1, LINC01465, DIP2A-IT1, TEX41, LINC00115, PCBP2-OT1, LINC00484, and HNF1A-AS1. By linking mRNA-miRNA and miRNA-lncRNA pairs via shared miRNAs, a ceRNA network comprising 30 regulatory axes was constructed (Fig. 7B). Many of these lncRNAs showed significant correlations with key infiltrating immune cells in gout (Fig. 7C).

3.6. Gene set enrichment analysis focus on CXCL8

Given its status as a top hub gene with the highest $\log_2$FC and its presence in the immune and ceRNA networks, *CXCL8* was selected for focused pathway analysis. GSEA was performed

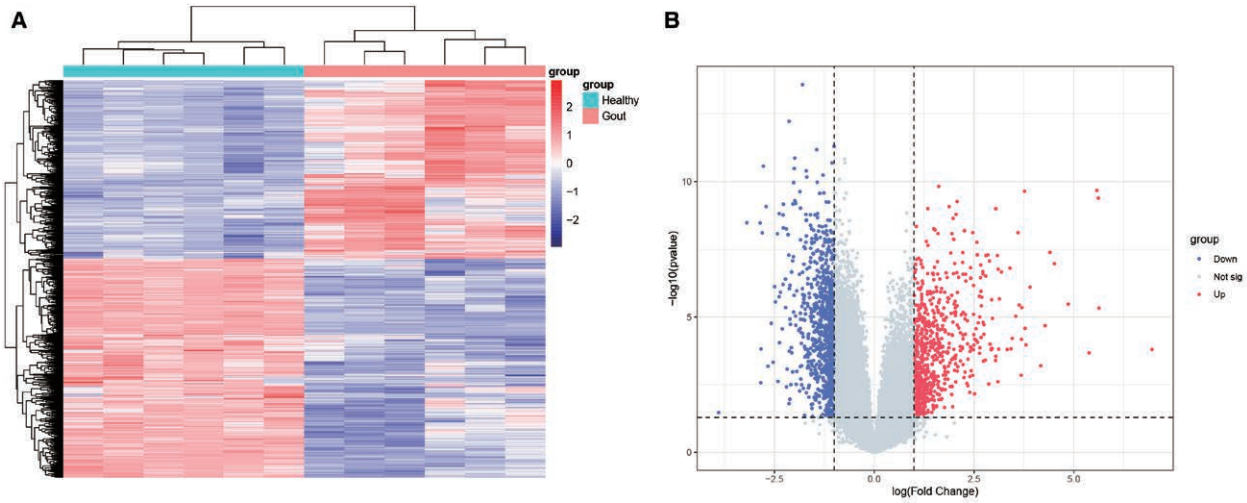

Figure 2. Visualization of differentially expressed genes (DEGs). (A) Heat map of DEGs. (B) Volcano map of DEGs. DEG = differentially expressed gene.

Table 1

The top 10 biological processes of GO_BP of DEGs.

GO_BP ID	Description	GeneRatio	*P*-value
GO:0031649	Heat generation	5/815	.000823493
GO:0035743	CD4-positive, alpha-beta T cell cytokine production	5/815	.000823493
GO:0050920	Regulation of chemotaxis	21/815	.00076708
GO:0002287	Alpha-beta T cell activation involved in immune response	10/815	.000765894
GO:0002293	Alpha-beta T cell differentiation involved in immune response	10/815	.000765894
GO:0002824	Positive regulation of adaptive immune response based on somatic recombination of immune receptors built from immunoglobulin superfamily domains	13/815	.000758396
GO:0032872	Regulation of stress-activated MAPK cascade	19/815	.000739635
GO:0033673	Negative regulation of kinase activity	22/815	.000705185
GO:0046328	Regulation of JNK cascade	15/815	.00068372
GO:0046637	Regulation of alpha-beta T cell differentiation	10/815	.000680978

DEG = differentially expressed genes, GO_BP = gene ontology biological process.

to investigate the signaling pathways associated with *CXCL8* expression in gout. The results confirmed that *CXCL8* remained primarily abundant in the NOD-like receptor signaling pathway, in addition to enrichment in the pentose phosphate pathway, Erbb signaling pathway, and tryptophan metabolism system (Fig. 8).

3.7. CXCL8 and NLRP3 inflammasome in hyperuricaemia-induced injury

To functionally validate the bioinformatic insights linking *CXCL8* to the NOD-like receptor pathway in a hyperuricaemic context, we established an in vitro model using human renal tubular epithelial cells (HK-2). Cells were treated with increasing concentrations of UA (0–40 mg/dL). The CCK-8 assay demonstrated that cell viability decreased gradually with increasing UA concentration, and the difference was statistically significant ($P < .05$; Fig. 9). Based on this, a treatment concentration of 10 mg/dL UA was selected for subsequent mechanistic experiments. Western blot analysis of this hyperuricaemic cell model revealed that NLRP3 inflammatory vesicles were overexpressed, showing increased levels of NLRP3, ASC, and pro-Caspase-1. Concurrently, *CXCL8* expression was also significantly upregulated. Statistical analysis confirmed that NLRP3 expression was statistically correlated with *CXCL8* (Fig. 10). These experimental findings directly corroborated the bioinformatics prediction, confirming the involvement of *CXCL8* in the NOD-like receptor signaling pathway within a hyperuricemia-induced injury model.

4. Discussion

This study constitutes the first application of an integrated approach combining differential gene expression analysis, functional enrichment analysis, and PPI network construction to elucidate the molecular mechanisms implicated in gout. A total of 1848 DEGs were identified, many of which are closely tied to immune response pathways and regulatory mechanisms, underscoring the significant role of immune dysregulation in gout pathogenesis. Through PPI network analysis, key hub genes – including *CXCL8*, *VEGFA*, *TNF*, *JUN*, and *IL4* – were identified. To further elucidate the functional roles and interactions of these genes, immune infiltration analysis, ceRNA network construction, and GSEA were performed. Additionally, the expression of critical regulatory factors associated with hyperuricemia was validated via in vitro assays. These results provide crucial insights into the molecular transition from hyperuricemia to gout and highlight potential therapeutic targets for intervention.

In this research, we successfully identified 1848 DEGs, comprising 830 upregulated and 1018 downregulated genes. Enrichment analysis confirmed a strong association of these DEGs with immune response and regulatory pathways, highlighting the immune system's essential role in gout pathology. KEGG analysis further pinpointed these DEGs as participants in several key inflammatory signaling pathways, such as the Toll-like receptor, NOD-like receptor, MAPK, and p53 pathways. This involvement suggests a fundamental contribution of these pathways to the inflammatory processes underpinning gout.

The PPI network and module analysis identified 5 pivotal genes: *TNF*, *JUN*, *CXCL8*, *VEGFA* (upregulated), and *IL-4* (downregulated). While these genes are well-known inflammatory cytokines, most have not been previously linked to the development of gout, making this a potentially novel discovery. To develop a comprehensive understanding of the dysregulation of inflammatory cells in gout, an immune infiltration analysis was conducted. Compared to healthy controls, patients with gout exhibited a higher proportion of activated mast cells and a reduced percentage of naïve CD4+ T cells, resting NK cells,

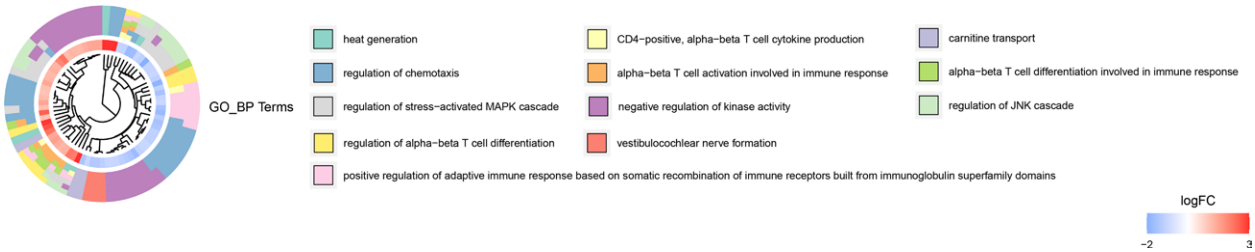

Figure 3. The top 12 biological processes of GO_BP of DEGs. DEG = differentially expressed gene, GO_BP = gene ontology biological process.

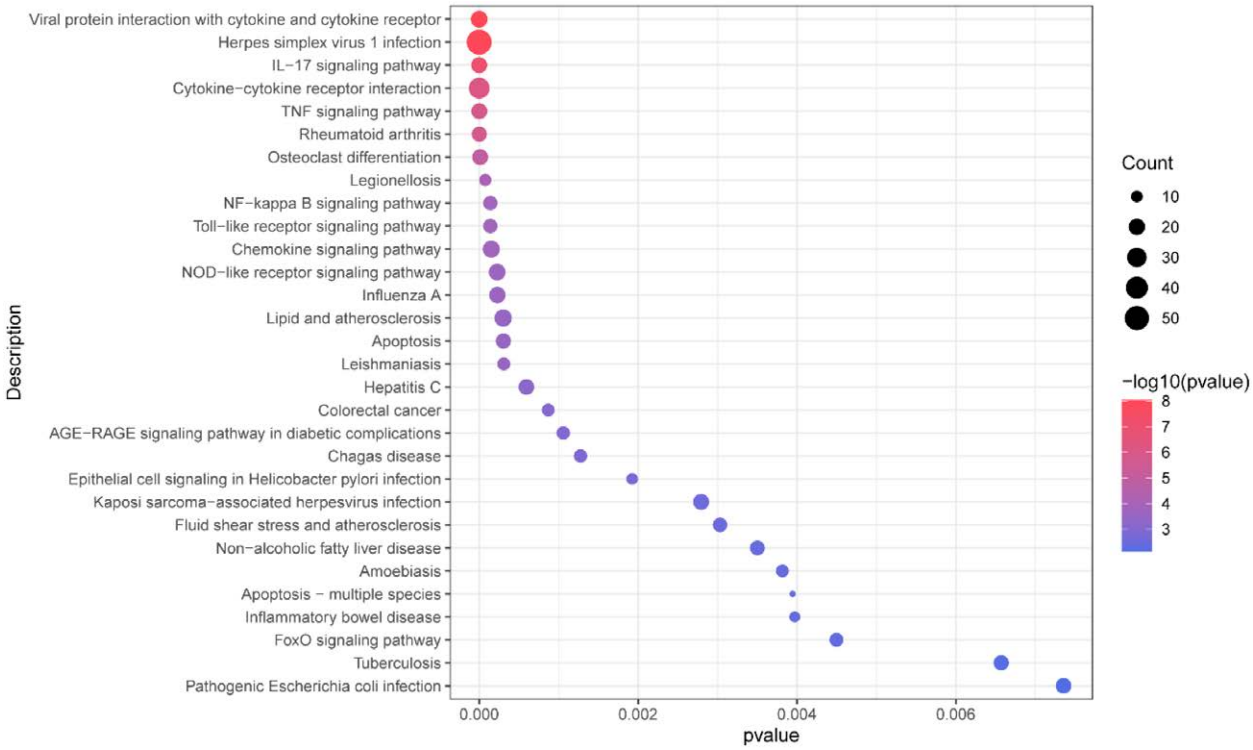

Figure 4. The top 30 signaling pathways of KEGG of DEGs. DEG = differentially expressed gene, KEGG = kyoto encyclopedia of genes and genomes.

M2 macrophages, and resting mast cells. Previous research has highlighted the crucial role of mast cells in the early inflammatory stages of acute gout.[30] Additionally, the dynamic balance of Th1/Th2 cells in CD4+ T cells has been implicated throughout all phases of gout inflammation.[31] In rat models of gout, M2 macrophages emerge early in the inflammatory process.[32] Our study further demonstrated statistically significant correlations between the core genes (*TNF*, *JUN*, *CXCL8*, *VEGFA*, and *IL-4*) and major infiltrating immune cells. Notably, activated mast cells were positively correlated with *CXCL8*, *JUN*, *VEGFA*, and *TNF* expression, suggesting that these genes are central to the dysregulation of inflammatory cells in gout and may function as key immunoregulatory hubs. To explore the interactive regulatory mechanisms in gout, we constructed a ceRNA network consisting of 30 axes, including notable interactions such as *CXCL8*/has-miR-1227-5p/LINC01465 and *JUN*/has-miR-92b-3p/HNF1A-AS1.

Interestingly, several long non-coding RNAs (LINC01433, KCTD21-AS1, HNF1A-AS1, and TEX41) showed significant positive correlations with activated mast cells, while others like LINC00115, DIP2A-IT1, and UCA1 were negatively correlated with naïve CD4+ T cells. Additionally, LINC01465 and LINC01433 were negatively correlated with M2 macrophages, and several lncRNAs exhibited negative correlations with resting NK cells and resting mast cells. These findings reinforce the hypothesis that the ceRNA network plays a critical role in the dysregulation of inflammatory cells in gout, providing new insights into potential immunoregulatory mechanisms. While ceRNA regulatory networks have been extensively studied in cancers and other inflammatory diseases, their role in gout, particularly in orchestrating immune cell dysregulationc, remains underexplored. Our construction of a *CXCL8*-centered ceRNA network, incorporating key lncRNAs such as LINC01465, HNF1A-AS1, and UCA1, provides a novel transcriptional regulatory perspective on gout pathogenesis. The significant correlations observed between these lncRNAs and immune cell subsets (e.g., activated mast cells and naïve CD4+ T cells) suggest that ceRNA interactions may serve as an important layer of post-transcriptional regulation in gout-related inflammation. This network not only highlights potential non-coding RNA biomarkers but also opens new avenues for understanding the integrated RNA-mediated regulatory landscape in gout.

We focused on *CXCL8* for in-depth analysis based on 2 critical observations. Firstly, *CXCL8* showed the most substantial $\log_2$FC among all HUB genes. Secondly, *CXCL8*, together with its upstream factors LINC01433, LINC01465, UCA1, PCBP2-OT1, and LINC00484, was significantly correlated with mast cell activation, indicating its possible crucial role in gout development. As a chemokine belonging to the CXC family, *CXCL8* is released mainly by neutrophils and

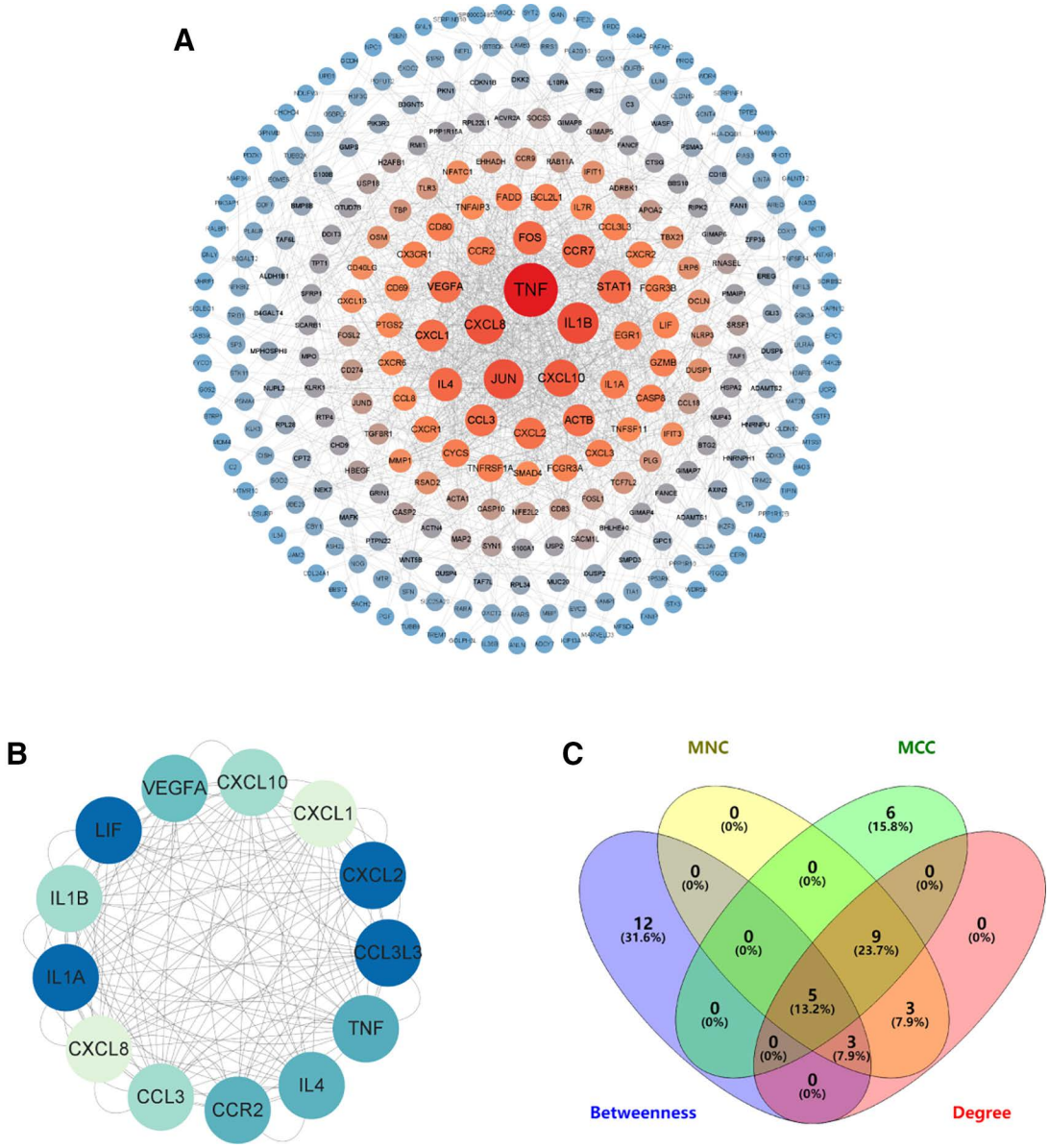

Figure 5. (A) PPI network of the DEGs. (B) Significant module selected from the PPI network. (C) Hub genes calculated by 4 algorithms. DEG = differentially expressed gene, PPI = protein–protein interaction.

Table 2

The top 5 hub genes.

Genes	Description	Degree	MCC	MNC	Betweenness	LogFC	Expression change
JUN	Jun proto-oncogene	30	17,932	30	24,562.61994	3.603974933	Upregulated
TNF	Tumor necrosis factor	50	5,13,916	50	22,394.5423	2.080435591	Upregulated
CXCL8	C-X-C motif chemokine ligand 8	30	5,44,987	30	6913.932019	5.577694379	Upregulated
IL4	Interleukin 4	22	52,533	22	6502.176116	-1.124800428	Downregulated
VEGFA	Vascular endothelial growth factor A	18	92,687	18	5305.104617	1.068061596	Upregulated

monocytes-macrophages. Its primary role is to recruit immune cells, including neutrophils, eosinophils, and lymphocytes, to sites of local inflammation, contributing to both inflammatory and allergic responses.[33] In addition to its chemotactic properties, *CXCL8* also stimulates neutrophils and basophils, dilates blood vessels, and enhances the proliferation of granulocytes and vascular cells. Moreover, *CXCL8* increases the production of IL-1, IL-6, and TNF-α, key pro-inflammatory cytokines, which can further drive the inflammatory process.[20] In gout, MSU crystal-induced stimulation of synovial endothelial cells significantly increases *CXCL8* mRNA levels, promoting neutrophil recruitment and aggregation, thus playing a key role in acute gouty inflammation.[34] This supports our findings that neutrophil-dependent inflammation is closely tied to *CXCL8* expression.[35] Additionally, in our in vitro model of hyperuricemia, we found that hyperuric acid elevated *CXCL8* expression in

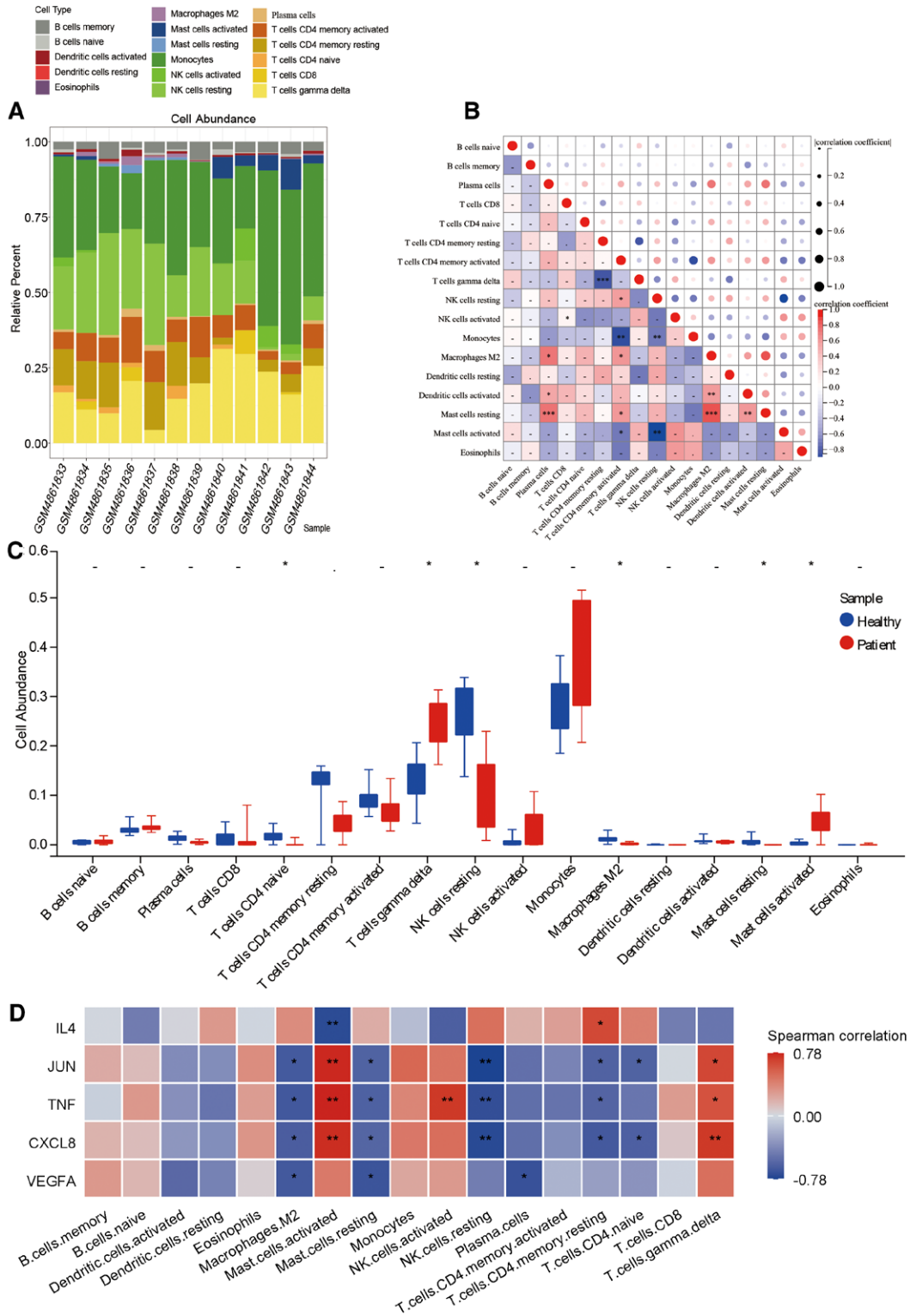

Figure 6. Immune infiltration analysis of GOUT. (A) The ratio of 17 immune cells of each sample of GOUT. (B) The correlation between each of immune cells. (C) The proportion of immune cells in GOUT and control. (D) The correlation between the hub gene and the immune cell.

renal tubular epithelial cells, a response significantly suppressed by allopurinol treatment ($P < .05$). These findings suggest that *CXCL8* may hold potential as a biomarker for diagnosing the progression of hyperuricemia to gout, though its clinical utility requires validation in larger, well-characterized patient cohorts.

According to GSEA results, the NOD-like receptor signaling pathway emerged as the primary pathway involved in *CXCL8* expression. Among the NOD-like receptors, the NLRP3 inflammasome is the most extensively studied and plays a crucial role as a sensor and receptor within the innate immune system.[36] NLRP3 expression is activated via the NF-κB pathway, where it forms a complex with the adaptor protein ASC and pro-caspase-1. This assembly enables pro-caspase-1 to undergo autocleavage, maturing into active caspase-1. Active caspase-1

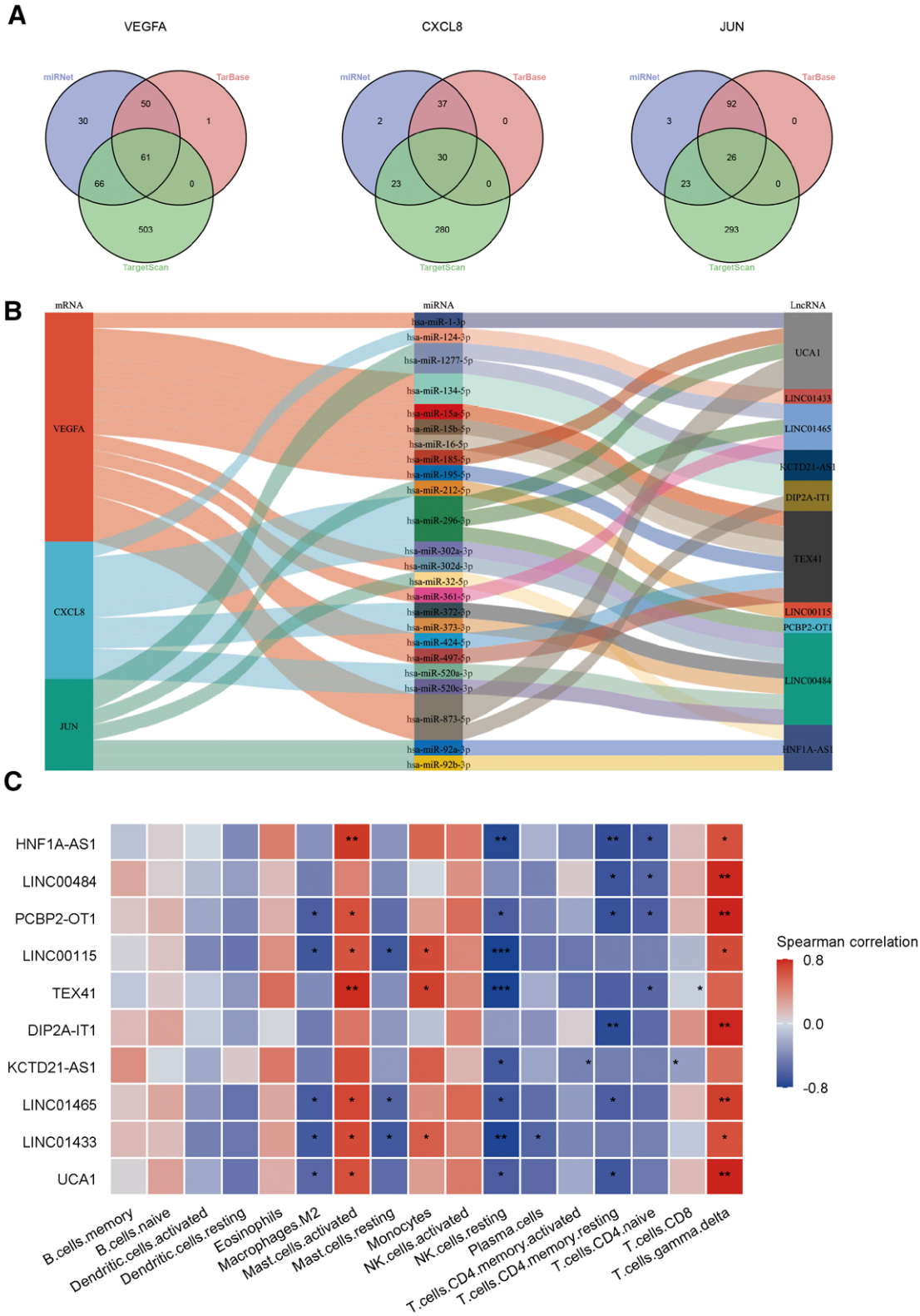

Figure 7. (A) The construction of the lncRNA–miRNA–mRNA ceRNA network of GOUT. Venn diagram of miRNAs targeting each hub gene. (B) The construction of the lncRNA–miRNA–mRNA ceRNA network of GOUT. The alluvial diagram of the ceRNA network. (C) The correlation between the lncRNA of ceRNA and immune cells. CeRNA = competing endogenous RNA.

then cleaves pro-IL-1β and pro-IL-18, converting them into their mature, pro-inflammatory forms (IL-1β and IL-18), which are released into the extracellular space, leading to local tissue inflammation or systemic inflammatory responses.[37] In an in vitro hyperuricemia cell model, we observed a statistically significant, UA-dependent increase in *CXCL8* expression and NLRP3 inflammasome-related proteins in renal tubular epithelial cells, as demonstrated by Western blot analysis. Additionally,

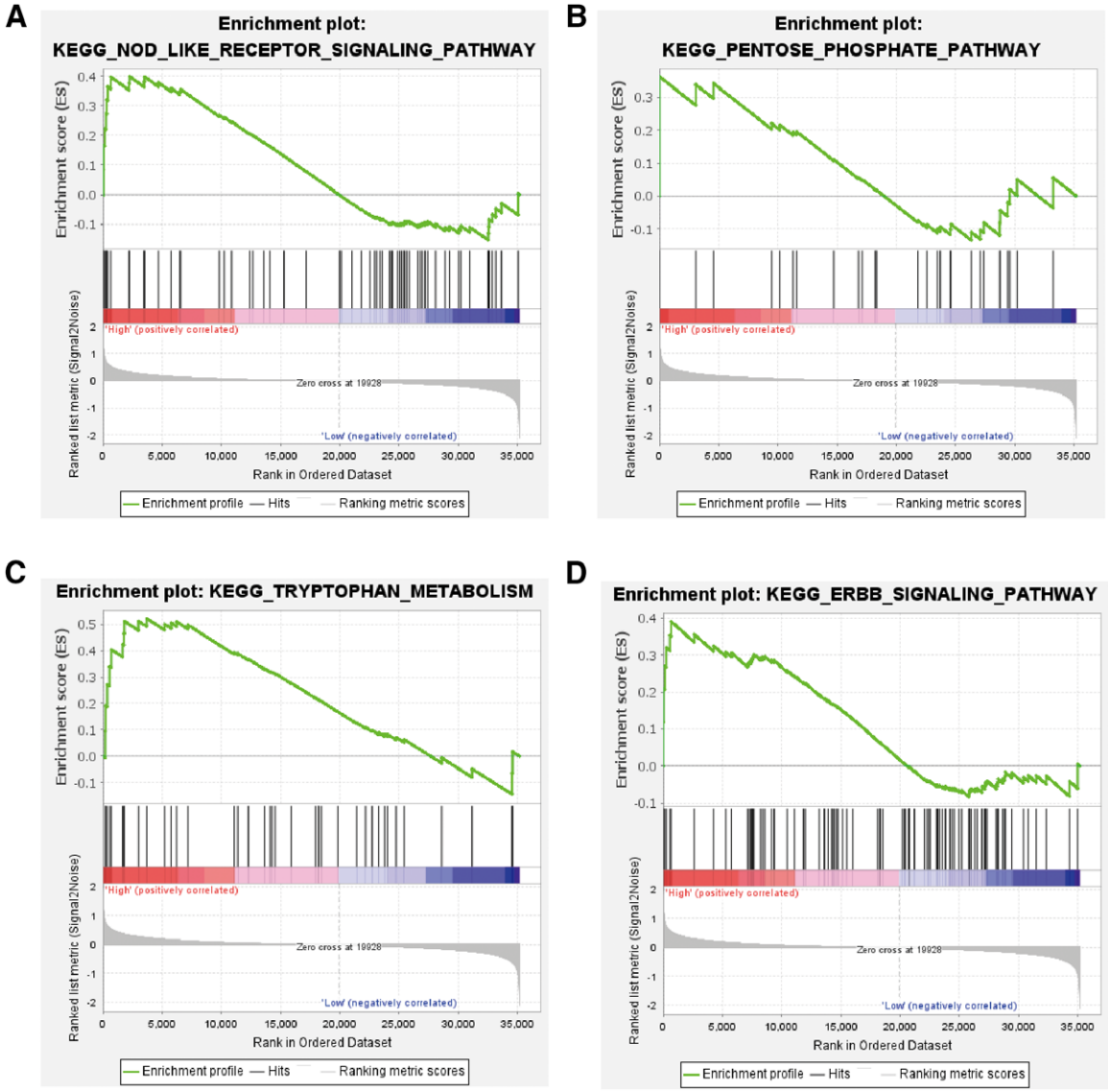

Figure 8. The GSEA of CXCL8. (A) NOD-like receptor signaling pathway. (B) Pentose phosphate pathway.(C) Tryptophan metabolism. (D) Erbb signaling pathway. CXCL8 = C-X-C motif chemokine ligand 8, GSEA = gene set enrichment analysis.

the expression levels of *CXCL8* and NLRP3 were significantly correlated ($P < .05$). These findings suggest that the NLRP3 inflammasome contributes to hyperuricemia-induced cellular inflammation and may be associated with *CXCL8* activation.

This study offers several distinct advantages, establishing itself as a leader in gout biomarker research while laying a robust foundation for future diagnostic and therapeutic advancements. First, the study adopts a systematic and multifaceted bioinformatics approach, incorporating differential gene expression analysis, pathway enrichment analysis, network construction, and PPI analysis. This integration sheds light on the underlying mechanisms behind the progression from hyperuricemia to gout from various angles. By employing multidimensional analyses, the study more accurately identifies key genes and signaling pathways closely associated with gout onset, bolstering both the scientific validity and reproducibility of its findings. Unlike studies that rely on a single analytical method, this diverse approach ensures that the results are more comprehensive and robust. Second, the study capitalizes on large-scale genomic data, enhancing its capability to pinpoint potential biomarkers. By leveraging publicly available data sources such as the GEO database, researchers were able to screen gout-associated genetic variants across a broad genetic background. The extensive data not only provided a strong basis for gene selection but also enhanced the generalizability of the results across different populations. Integrating large datasets also gave researchers deeper insights into molecular mechanisms, especially concerning under-explored genes and pathways. Compared to traditional single-experiment approaches, this data-driven methodology greatly improved the accuracy and scope of biomarker identification. Third, the study employs a rigorous multi-level validation process, ensuring the reliability and verifiability of its results. After identifying candidate biomarkers, the research team conducted preliminary validations through experiments like Western blot assays to confirm differential gene expression. Additionally, functional assays, such as cell proliferation tests, provided further support for exploring the specific roles of these genes in gout. This comprehensive validation – from bioinformatics predictions to experimental validation – ensured scientific rigor and laid clear pathways for future in-depth research. The thoroughness of this validation framework significantly strengthened the study's credibility and set the stage for further laboratory and clinical investigations. Moreover, the study's comprehensiveness and innovative methodology make it

highly promising for clinical translation. Beyond bioinformatics screening, the study explored the clinical applicability of biomarkers through laboratory experiments, ensuring the practical value of its findings. This systematic approach – spanning bioinformatics analysis, experimental validation, and clinical application – ensured that the study's contributions extended beyond theoretical research to practical clinical relevance. For instance, some genetic markers identified in the study hold promise for the development of early diagnostic tools that could help clinicians distinguish hyperuricemia patients at higher risk of developing gout, allowing for personalized interventions. Additionally, the discovery of these markers may guide future drug development, providing potential targets for innovative therapies. In conclusion, this study not only demonstrates methodological rigor and innovation but also excels in data breadth, validation strategies, and clinical translation potential. Through its multi-level analysis and experimental validation, it offers new insights into the mechanisms driving the transition from hyperuricemia to gout and lays the groundwork for future therapies. Further experimental and clinical investigations will build upon this foundation, paving the way for significant advances in the diagnosis and treatment of gout.

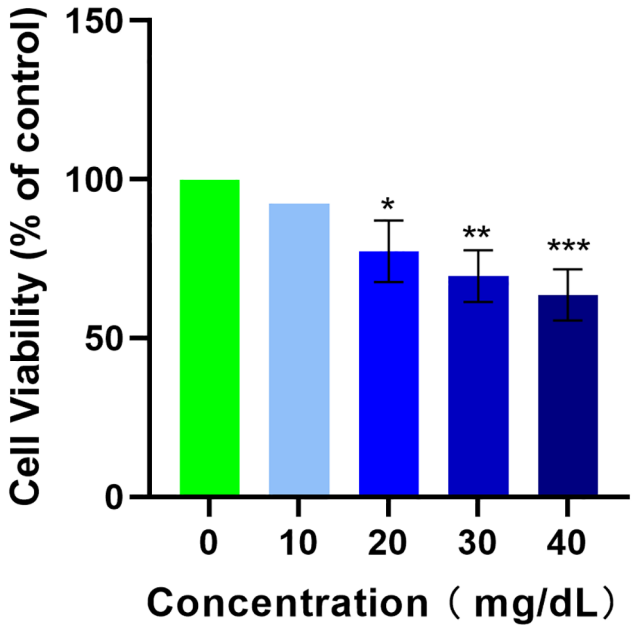

Figure 9. Screening of multi-gradient-soluble UA concentration (n = 10 each group). *P < .05 and **P < .01 versus control. UA = uric acid.

Despite the valuable insights provided by our bioinformatics analysis in identifying DEGs and pathways in gout, several limitations must be acknowledged, which could affect the generalizability and clinical translation of the findings. First, the analysis relied heavily on publicly available datasets, where data quality and completeness may vary. Incomplete annotations or inconsistencies across datasets could introduce potential biases, impacting the accuracy of the results. Additionally, the study primarily focused on transcriptomic data, which offers a snapshot of gene expression at a given time point. However, gout is a dynamic disease influenced by both genetic and environmental factors, and this static approach may not fully capture the complex gene-environment interactions or temporal changes involved in disease progression. Another limitation is the reliance on gene expression data from peripheral blood or synovial tissues, which, while relevant to systemic or localized inflammation in gout, may not fully represent the disease's impact on other relevant tissues or cell types. Tissue-specific gene regulation, especially in organs affected by gout such as the kidneys, could provide a more comprehensive understanding of the disease mechanisms. The homogeneity of the data in terms of racial and geographic backgrounds also raises concerns regarding the generalizability of the findings. Most of the analyzed data were derived from individuals of a specific ancestry, potentially limiting the applicability of the results to more diverse populations. Genetic variation across different

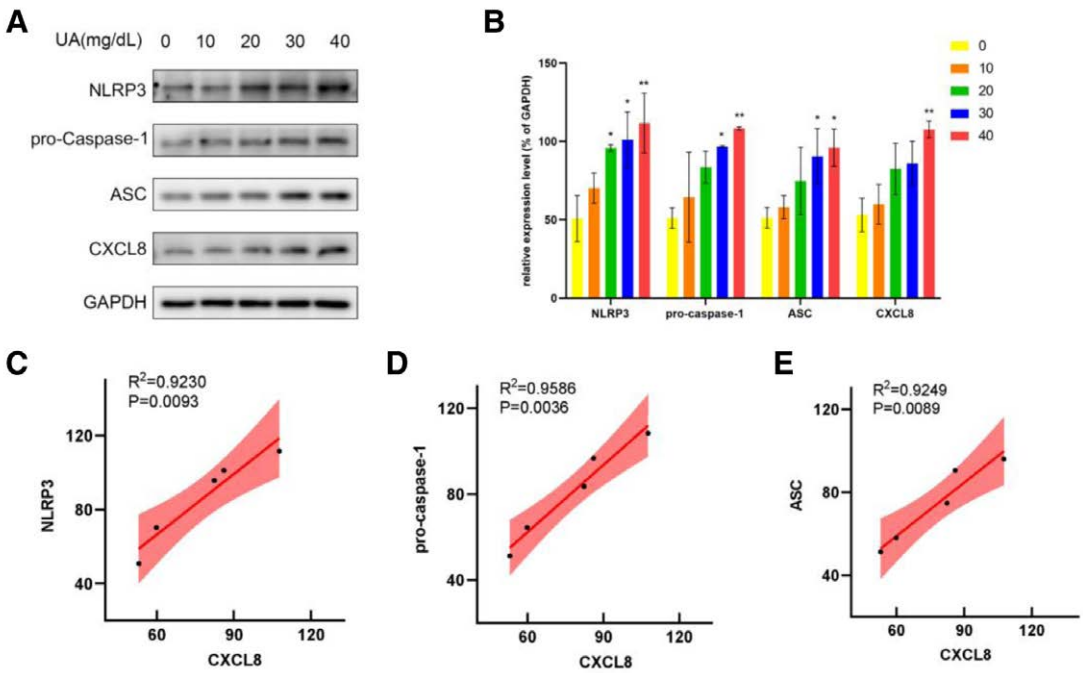

Figure 10. (A) Human HK-2 cells were treated with an increasing concentration of UA for 48 hours, and the expression levels of NLRP3 and CXCL8 in vitro experiment. (B) GAPDH protein expression was determined as a control for equal loading. *P < .05, **P < .01. (C) The correlation between NLRP3 and CXCL8. (D) The correlation between pro-caspase-1 and CXCL8. (E) The correlation between ASC and CXCL8. CXCL8 = C-X-C motif chemokine ligand 8, NLRP3 = NOD-like receptor family pyrin domain containing 3, UA = uric acid.

ethnic groups may influence gene expression and susceptibility to gout, making it necessary for future studies to include a broader range of populations to ensure the results are more universally relevant. Additionally, the sample size was relatively small, and all participants were male, which could further limit the generalizability of the findings, as gender differences in disease mechanisms or gene expression may not have been captured. Our bioinformatics analysis was based on a single dataset (GSE160170). Although we performed experimental validation to support our findings, the lack of cross-validation with independent transcriptomic cohorts limits the generalizability of our bioinformatics results. Future studies incorporating multiple datasets are needed to confirm the robustness of the identified DEGs and pathways. Most importantly, the limited sample size and lack of validation in an independent clinical cohort preclude definitive conclusions regarding the robust diagnostic utility of *CXCL8*. Our findings position *CXCL8* as a strong candidate for further investigation, but its translation into a clinically applicable biomarker necessitates rigorous validation in larger, multi-center studies involving diverse patient populations. Therefore, while this study lays the groundwork for understanding key molecular mechanisms in gout, further research is needed to address these limitations and bring potential findings closer to clinical application.

5. Conclusion

From the GSE160170 dataset, we identified 5 key genes – *TNF*, *JUN*, *IL4*, *CXCL8*, and *VEGFA* – which play crucial roles in the immune response and the dysregulation of inflammatory cells in gout. Notably, *CXCL8* and its ceRNA axis may be responsible for the activation of mast cells, potentially through the NOD-like receptor signaling pathway. This suggests that *CXCL8* and its associated molecules warrant further investigation as potential diagnostic markers for the progression from hyperuricaemia to gout. Our findings offer preliminary insights into gout pathophysiology and highlight candidate targets for future therapeutic strategies. Additionally, our findings provide new insights into the pathophysiology of gout and open avenues for novel therapeutic interventions.

Author contributions

Conceptualization: Chao Zhang.
Data curation: Chao Zhang, Chunhong Liu, Xiaoming Yang, Xin Lin, Miao Wang.
Funding acquisition: Yanlang Yang.
Investigation: Chao Zhang.
Methodology: Chao Zhang.
Visualization: Chao Zhang.
Writing – original draft: Chao Zhang.
Writing – review & editing: Yanlang Yang.

References

[1] Richette P, Doherty M, Pascual E, et al. 2018 updated European League Against Rheumatism evidence-based recommendations for the diagnosis of gout. Ann Rheum Dis. 2020;79:31–8.
[2] Stamp LK, Frampton C, Morillon MB, et al. Association between serum urate and flares in people with gout and evidence for surrogate status: a secondary analysis of two randomised controlled trials. Lancet Rheumatol. 2022;4:e53–60.
[3] Tin A, Marten J, Kuhns VL H, et al. Target genes, variants, tissues and transcriptional pathways influencing human serum urate levels. Nat Genet. 2019;51:1459–74.
[4] Dalbeth N, Phipps-Green A, Frampton C, Neogi T, Taylor WJ, Merriman TR. Relationship between serum urate concentration and clinically evident incident gout: an individual participant data analysis. Ann Rheum Dis. 2018;77:1048–52.
[5] Kapetanovic MC, Nilsson P, Turesson C, Englund M, Dalbeth N, Jacobsson L. The risk of clinically diagnosed gout by serum urate levels: results from 30 years follow-up of the Malmö Preventive Project cohort in southern Sweden. Arthritis Res Ther. 2018;20:190.
[6] Dalbeth N, Gosling AL, Gaffo A, Abhishek A. Gout. Lancet. 2021;397:1843–55.
[7] Major TJ, Dalbeth N, Stahl EA, Merriman TR. An update on the genetics of hyperuricaemia and gout. Nat Rev Rheumatol. 2018;14:341–53.
[8] Bardin T, Richette P. Definition of hyperuricemia and gouty conditions. Curr Opin Rheumatol. 2014;26:186–91.
[9] Kuo C-F, Grainge MJ, See L-C, et al. Familial aggregation of gout and relative genetic and environmental contributions: a nationwide population study in Taiwan. Ann Rheum Dis. 2015;74:369–74.
[10] Gill D, Cameron AC, Burgess S, et al. Urate, blood pressure, and cardiovascular disease: evidence from mendelian randomization and meta-analysis of clinical trials. Hypertension. 2021;77:383–92.
[11] Connaughton DM, Hildebrandt F. Personalized medicine in chronic kidney disease by detection of monogenic mutations. Nephrol Dial Transplant. 2020;35:390–7.
[12] Lanktree MB, Iliuta I-A, Haghighi A, Song X, Pei Y. Evolving role of genetic testing for the clinical management of autosomal dominant polycystic kidney disease. Nephrol Dial Transplant. 2019;34:1453–60.
[13] Harris PC, Torres VE. Genetic mechanisms and signaling pathways in autosomal dominant polycystic kidney disease. J Clin Invest. 2014;124:2315–24.
[14] Hasin Y, Seldin M, Lusis A. Multi-omics approaches to disease. Genome Biol. 2017;18:83.
[15] Tsagiopoulou M, Gut IG. Machine learning and multi-omics data in chronic lymphocytic leukemia: the future of precision medicine? Front Genet. 2023;14:1304661.
[16] Afinogenova Y, Danve A, Neogi T. Update on gout management: what is old and what is new. Curr Opin Rheumatol. 2022;34:118–24.
[17] Cambier S, Gouwy M, Proost P. The chemokines CXCL8 and CXCL12: molecular and functional properties, role in disease and efforts towards pharmacological intervention. Cell Mol Immunol. 2023;20:217–51.
[18] de Oliveira S, Rosowski EE, Huttenlocher A. Neutrophil migration in infection and wound repair: going forward in reverse. Nat Rev Immunol. 2016;16:378–91.
[19] Xiong X, Liao X, Qiu S, et al. CXCL8 in Tumor Biology and Its Implications for Clinical Translation. Front Mol Biosci. 2022;9:723846.
[20] Ha H, Debnath B, Neamati N. Role of the CXCL8-CXCR1/2 axis in cancer and inflammatory diseases. Theranostics. 2017;7:1543–88.
[21] Huntley RP, Harris MA, Alam-Faruque Y, et al. A method for increasing expressivity of Gene Ontology annotations using a compositional approach. BMC Bioinf. 2014;15:155.
[22] Kanehisa M, Goto S. KEGG: kyoto encyclopedia of genes and genomes. Nucleic Acids Res. 2000;28:27–30.
[23] Szklarczyk D, Gable AL, Lyon D, et al. STRING v11: protein-protein association networks with increased coverage, supporting functional discovery in genome-wide experimental datasets. Nucleic Acids Res. 2019;47:D607–13.
[24] Chin C-H, Chen S-H, Wu H-H, Ho C-W, Ko M-T, Lin C-Y. cytoHubba: identifying hub objects and sub-networks from complex interactome. BMC Syst Biol. 2014;8(Suppl 4):S11.
[25] Chen B, Khodadoust MS, Liu CL, Newman AM, Alizadeh AA. Profiling tumor infiltrating immune cells with CIBERSORT. Methods Mol Biol. 2018;1711:243–59.
[26] Mitteer DR, Greer BD, Randall KR, Briggs AM. Further evaluation of teaching behavior technicians to input data and graph using graphpad prism. Behav Anal (Wash D C). 2020;20:81–93.
[27] Shi Y, Yang F, Wei S, Xu G. Identification of key genes affecting results of hyperthermia in osteosarcoma based on integrative ChIP-Seq/TargetScan analysis. Med Sci Monit. 2017;23:2042–8.
[28] Chang L, Zhou G, Soufan O, Xia J. miRNet 2.0: network-based visual analytics for miRNA functional analysis and systems biology. Nucleic Acids Res. 2020;48:W244–51.
[29] Subramanian A, Tamayo P, Mootha VK, et al. Gene set enrichment analysis: a knowledge-based approach for interpreting genome-wide expression profiles. Proc Natl Acad Sci U S A. 2005;102:15545–50.
[30] Reber LL, Marichal T, Sokolove J, et al. Contribution of mast cell-derived interleukin-1β to uric acid crystal-induced acute arthritis in mice. Arthritis Rheumatol. 2014;66:2881–91.
[31] Zhao L-J, Wang H, Gao H-Y, Wang J, Gao C, Li X-F. Increase in different peripheral effector T subsets in acute and chronic gout. Transpl Immunol. 2022;76:101763.

[32] Zhao L, Ye W, Zhu Y, et al. Distinct macrophage polarization in acute and chronic gout. Lab Invest. 2022;102:1054–63.
[33] Hou Y, Huttenlocher A. Advancing chemokine research: the molecular function of CXCL8. J Clin Invest. 2024;134:e180984.
[34] Li D, Yuan S, Deng Y, et al. The dysregulation of immune cells induced by uric acid: mechanisms of inflammation associated with hyperuricemia and its complications. Front Immunol. 2023;14:1282890.
[35] Kim K-W, Kim B-M, Lee K-A, Kim H-S, Lee S-H, Kim H-R. Reciprocal interaction between macrophage migration inhibitory factor and interleukin-8 in gout. Clin Exp Rheumatol. 2019;37:270–8.
[36] Kelley N, Jeltema D, Duan Y, He Y. The NLRP3 inflammasome: an overview of mechanisms of activation and regulation. Int J Mol Sci . 2019;20:3328.
[37] Shao B-Z, Xu Z-Q, Han B-Z, Su D-F, Liu C. NLRP3 inflammasome and its inhibitors: a review. Front Pharmacol. 2015;6:262.